Photochemical & Photobiological Sciences c2pp05351a

1

Optical and electrochemical properties of hydrogen-bonded phenol-pyrrolidino[60]fullerenes

Gary F. Moore, Jackson D. Megiatto, Jnr, Michael Hambourger, Miguel Gervaldo, Gerdenis Kodis, Thomas A. Moore*, Devens Gust* and Ana L. Moore*

Pyrrolidino[60]fullerenes act as built in proton-accepting units that influence the potential of the phenoxyl radical–phenol couple in photochemically active redox pairs.

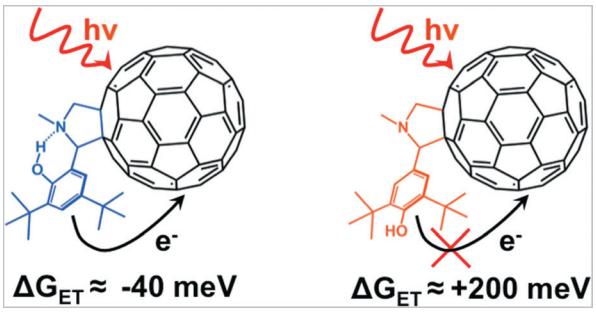

Please check this proof carefully. **Our staff will not read it in detail after you have returned it.**

Translation errors between word-processor files and typesetting systems can occur so the whole proof needs to be read. Please pay particular attention to: tabulated material; equations; numerical data; figures and graphics; and references. If you have not already indicated the corresponding author(s) please mark their name(s) with an asterisk. Please e-mail a list of corrections or the PDF with electronic notes attached – do not change the text within the PDF file or send a revised manuscript.

Please bear in mind that minor layout improvements, e.g. in line breaking, table widths and graphic placement, are routinely applied to the final version.

We will publish articles on the web as soon as possible after receiving your corrections; no late corrections will be made.

Please return your **final** corrections, where possible within **48 hours** of receipt, by e-mail to: pps@rsc.org

Reprints—Electronic (PDF) reprints will be provided free of charge to the corresponding author. Enquiries about purchasing paper reprints should be addressed via: http://www.rsc.org/publishing/journals/guidelines/paperreprints/. Costs for reprints are below:

Reprint costs

	Cost (per 50 copies)	
No of pages	**First**	**Each additional**
2–4	£225	£125
5–8	£350	£240
9–20	£675	£550
21–40	£1250	£975
>40	£1850	£1550

Cost for including cover of journal issue:
£55 per 50 copies

The Royal Society of Chemistry

Proofs for Correction pps

Dear Author,

Paper No. c2pp05351a

Please check the proofs of your paper carefully, paying particular attention to the numerical data, tables, figures and references.

When answering the queries below please ensure that any changes required are clearly marked **on the proof**. There is no need to e-mail your answers to the queries separately from the rest of your proof corrections.

Editor's queries are marked like this [Q1, Q2, …], and for your convenience line numbers are indicated like this [5, 10, 15, …].

Many thanks for your assistance.

Query	Remarks
Q1 For your information: You can cite this article before you receive notification of the page numbers by using the following format: (authors), Photochem. Photobiol. Sci., (year), DOI: 10.1039/c2pp05351a.	
Q2 Please carefully check the spelling of all author names. This is important for the correct indexing and future citation of your article. No late corrections can be made.	
Q3 AQ: Two different terms have been used "$Tyr_{(Z)}$ or $Tyr_{(z)}$". Please check this carefully and indicate any changes required here.	
Q4 Ref. 19c: Please provide the following details: volume number.	
Q5 Ref. 31(a) and 31(b) appear to be identical. Do you wish to replace either of these with a different reference? also check ref 31b, id changed to 31c which was repeated twice.	

Photochemical & Photobiological Sciences

Dynamic Article Links

Cite this: DOI: 10.1039/c2pp05351a

www.rsc.org/pps

PAPER

Optical and electrochemical properties of hydrogen-bonded phenol-pyrrolidino[60]fullerenes

Gary F. Moore, Jackson D. Megiatto, Jnr, Michael Hambourger, Miguel Gervaldo, Gerdenis Kodis, Thomas A. Moore,* Devens Gust* and Ana L. Moore*

Received 19th October 2011, Accepted 2nd January 2012
DOI: 10.1039/c2pp05351a

We report the photophysical and electrochemical properties of phenol–pyrrolidino[60]fullerenes **1**, and **2**, in which the phenol hydroxyl group is *ortho* and *para* to the pyrrolidino group, respectively, as well as those of a phenyl–pyrrolidino[60]fullerene model compound, **3**. For the *ortho* analog **1**, the presence of an intramolecular hydrogen bond is supported by ^{1}H NMR and FTIR characterization. The redox potential of the phenoxyl radical–phenol couple in this architecture is 240 mV lower than that observed in the associated *para* compound **2**. Further, the C_{60} excited-state lifetime of the hydrogen-bonded compound **1** in benzonitrile is 260 ps, while the corresponding lifetime for **2** is identical to that of the model compound **3** at 1.34 ns. Addition of excess organic acid to a benzonitrile solution of **1** gives rise to a new species, **4**, with an excited-state lifetime of 1.40 ns. In nonpolar aprotic solvents such as toluene, all three compounds have a C_{60} excited-state lifetime of ~1.34 ns. These results suggest that the presence of an intramolecular H-bond in **1** poises the potential of phenoxyl radical–phenol redox couple at a value that it is thermodynamically capable of reducing the photoexcited fullerene. This is not the case for the *para* analog **2** nor is it the case for the protonated species **4**. This work illustrates that in addition to being used as light activated electron acceptors, pyrrolidino fullerenes are also capable of acting as built in proton-accepting units that influence the potential of an attached donor when organized in an appropriate molecular design.

1. Introduction

Proton coupled electron transfer (PCET) is a fundamental aspect of many biological electron transfer reactions.[1–13] In the water oxidizing enzyme Photosystem II (PSII)[14] a tyrosine residue (Tyr_z), hydrogen bonded to a nearby histidine moiety (His190), forms a redox-active pair that mediates electron transfer between the primary chlorophyll donor (P_{680}) and the Mn_4CaO_5 oxygen-evolving complex (OEC). Photoexcitation of PSII produces the radical cation $P_{680}^{\cdot+}$. In turn, $P_{680}^{\cdot+}$ is reduced by the Tyr_z–His190 pair. In this process, formation of the tyrosyl radical is coupled to release of the phenolic proton to an adjacent base (most likely the His190 imidazole residue). The neutral tyrosyl radical ($Tyr_z^{\cdot}$) is then reduced by the OEC, resulting in activation of this complex for water splitting reactions.[1,3] The coupling of the proton and electron transfer chemistry is a crucial feature of the photosynthetic process and is imperative for achieving the appropriate redox leveling necessary to drive the multi-electron catalytic processes with photogenerated oxidizing equivalents.

Aspects of PCET may also prove essential for developing efficient interfaces between light absorbers and redox-active–catalytic components in artificial photosynthesis. Likewise, serious efforts have been devoted to understanding the kinetic details and mechanistic implications of PCET reactions in simplified model systems.[15–21] A typical molecular design of a model system consists of an intra- or inter-molecular hydrogen bond between a phenolic proton and the lone pair electrons of an organic base. Pyridine, imidazole, and amines have been investigated as proton acceptors in both electrochemically- and light-driven redox reactions. Despite this progress, experimental and theoretical data remain limited.

We have previously reported[21a] a photochemically active model of the Tyr_Z–His190-chlorophyll complex of PSII. In this system, a hydrogen-bonded phenol–benzimidazole pair (PhOH–Bi) is covalently attached to a bis(pentafluorophenyl)–porphyrin (PF_{10}) that is adsorbed at the surface of titanium dioxide nanoparticles (TiO_2). Light excitation of the porphyrin triggers a sequence of electron and proton transfer reactions that ultimately yields the $PhO^{\cdot}$–BiH^{+}–PF_{10}–$TiO_2^{\cdot-}$ state, which is characterized by a neutral phenoxyl radical, a protonated

Center for Bioenergy and Photosynthesis, Department of Chemistry and Biochemistry, Arizona State University, Tempe, Arizona 85287-1604, USA. E-mail: gust@asu.edu, tmoore@asu.edu, amoore@asu.edu
†Current address: Joint Center for Artificial Photosynthesis, Lawrence Berkeley National Laboratory, Berkeley CA 94720.
‡Current address: A. R. Smith Department of Chemistry, Appalachian State University, Boone, NC 28608.
§Current address: Departamento de Química Facultad de Ciencias Exactas, Físico-Químicas y Naturales Universidad Nacional de Río Cuarto, Río Cuarto, Argentina, 5800.

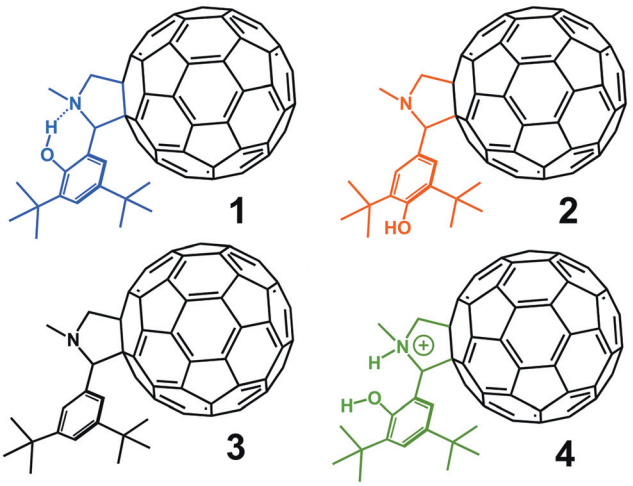

Fig. 1 Phenol–pyrrolidino[60]fullerene compounds investigated in the present work.

benzimidazole moiety, and an electron delocalized across the TiO_2 conduction band. Acid–base titration experiments[21b] indicate that an ionizable proton controls the electrochemical potential of the phenolic species, while maintaining the chemical reversibility of the PhOH–Bi component.

In this contribution, we extend our investigation of photoinduced PCET reactions in artificial systems to include a molecular architecture in which the phenol moiety is covalently attached to a pyrrolidino[60]fullerene (Fig. 1). In **1** (PhOH–PyrC_{60}), the phenolic unit is positioned to form an intramolecular hydrogen bond with the basic nitrogen lone pair electrons of the pendant pyrrolidino[60]fullerene. Light excitation of the fullerene triggers a PCET reaction, presumably forming a charge-separated radical pair composed of a neutral phenoxyl radical and a zwitterionic pyrrolidino[60]fullerene group (PhO$^{\cdot}$–Pyr$H^{+}C_{60}^{\cdot-}$). The behavior of the hydrogen-bonded construct **1** is compared to that of analogs **2**, **3**, and **4** in which the intramolecular hydrogen bond is either absent or disrupted.

2 Experimental section

2.1 Materials

Trifluoroacetic acid, 2,4-di-*tert*-butylphenol and *N*-methylglycine were purchased from Alfa Aesar and Acros. Aldehyde precursors 3,5-di-*tert*-butyl-4-hydroxybenzaldehyde and 3,5-di-*tert*-butylbenzaldehyde were purchased from Aldrich. All chemicals were used without further purification. Solvents were obtained from EM Science. Toluene was distilled over CaH_2, and dichloromethane was distilled over potassium carbonate. All solvents were stored over the appropriate molecular sieves prior to use. Thin layer chromatography (TLC) was performed with silica gel coated glass plates from Analtech. Column chromatography was carried out using Silicycle silica gel 60 with 230–400 mesh.

2.2 Spectroscopic measurements

The ^{1}H-NMR spectra were recorded on a Varian spectrometer at 400 MHz. NMR samples were prepared in deuteriochloroform with tetramethylsilane as an internal reference using a Wilmad 528-PP 5 mm NMR tube. In some cases, carbon disulfide was included in the NMR solvent to enhance solubility. Mass spectra were obtained with a matrix-assisted laser desorption–ionization time-of-flight spectrometer (MALDI-TOF), using (1*E*,3*E*)-1,4-diphenylbuta-1,3-diene (DPB), cyano-4-hydroxycinnamic acid (CCA) or terthiophene as a matrix. The reported mass is of the most abundant isotopic ratio observed. To facilitate comparison, calculated values of the expected most abundant isotopic ratio are listed after the experimental result. Steady-state UV-Vis absorption spectra were measured on a Shimadzu UV-3101PC UV-Vis-NIR spectrometer. FTIR spectra were measured on a Thermo Scientific Nicolet 380 FT-IR spectrometer with an attenuated total reflectance head by evaporating a dichloromethane solution of the sample onto the sample compartment base plate. Steady-state fluorescence spectra were measured using a Photon Technology International MP-1 spectrometer and corrected for detection system response. Excitation was provided by a 75 W xenon-arc lamp and single grating monochromator. Fluorescence was detected 90° to the excitation beam *via* a single grating monochromator and an R928 photomultiplier tube having S-20 spectral response and operating in the single-photon-counting mode. Time-resolved fluorescence decay measurements were performed by the time-correlated single-photon-counting method. The excitation source was a mode-locked Ti : sapphire laser (Spectra Physics, Millennia-pumped Tsunami) with a 130 fs pulse duration operating at 80 MHz. The laser output was sent through a frequency doubler and pulse selector (Spectra Physics Model 3980) to obtain 370–450 nm pulses at 4 MHz. Fluorescence emissions were detected at the magic angle using a double grating monochromator (Jobin Yvon Gemini-180) and a microchannel plate photomultiplier tube (Hamamatsu R3809U-50). The instrument response function was 35–55 ps. The spectrometer was controlled by software written in the LabView programming language[22] and data acquisition was done using a single–photon-counting card (Becker-Hickl, SPC-830). Data analysis was carried out using locally written software (ASUFIT) developed in a MATLAB environment (Mathworks Inc.). Data were fitted as a sum of exponential decays, which were reconvoluted with the appropriate instrument response function. Goodness of fit was established by examination of residuals and the reduced χ^2 value, which was <1.20 for all kinetics reported. The data were obtained in benzonitrile unless otherwise specified. When noted, the spectra have been normalized to facilitate comparison of the data. *In situ* generation of the protonated form of the phenol–pyrrolidinofullerene was achieved by the addition of trifluoroacetic acid (TFA). For acid–base titrations, dilution series of TFA in benzonitrile were used.

Cyclic voltammetry was performed with a CHI 650C potentiostat (CH Instruments) using a glassy carbon (3 mm diameter) or platinum (1.6 mm diameter) disc working electrode, a platinum gauze counter electrode, and a silver wire pseudoreference electrode in a conventional three-electrode cell. Benzonitrile, distilled from phosphorus pentoxide, was used as the solvent for electrochemical measurements. The supporting electrolyte was 0.10 M tetrabutylammonium hexafluorophosphate. The solution was deoxygenated by bubbling with argon. Experiments in acidified benzonitrile were performed by adding trifluoroacetic acid (from stock solutions in the same solvent) to a final

concentration as high as 0.5 M. The working electrode was cleaned between experiments by polishing with alumina (50 nm dia.) slurry, followed by solvent rinses. The concentration of the electroactive compound was maintained between 4×10^{-4} and 8×10^{-4} M. The potential of the pseudoreference electrode was determined using the ferrocenium–ferrocene redox couple as an internal standard (with E_m taken as 0.45 V *vs.* SCE in benzonitrile). The voltammograms were recorded at 100 mV s^{-1}. Cyclic voltammograms obtained at a glassy carbon working electrode have had the baseline subtracted, using a baseline recorded under comparable conditions in the absence of the electroactive species.

2.3 Synthesis

3,5-Di-*tert*-butyl-2-hydroxybenzaldehyde:[23]. A solution of commercially available 2,4-di-*tert*-butylphenol (4.12 g, 20 mmol, 1 equiv.), hexamethylenetetramine (5.66 g, 40 mmol, 2 equiv.) and trifluoroacetic acid (20 mL) was heated at reflux for 6 h. The reaction was quenched while hot with a 33% (v/v) aqueous H_2SO_4 solution (20 mL) and the resulting mixture was allowed to cool to room temperature with stirring. The crude product was extracted with diethyl ether (3 × 50 mL), and the extract was neutralized with a saturated aqueous solution of sodium bicarbonate (2 × 100 mL) and finally washed with water (3 × 100 mL). The organic phase was dried over sodium sulfate, filtered through paper and concentrated under reduced pressure. Final purification was achieved by column chromatography (SiO_2), using hexanes–EtOAc (9 : 1, v/v) as eluent to afford the title compound as a colorless solid in 35% yield (1.64 g). ^{1}H NMR (400 MHz, $CDCl_3$, δ ppm): 11.80 (s, 1H, OH); 9.88 (s, 1H, CHO); 7.82 (d, J = 1.7 Hz, 1H, ArH); 7.58 (d, J = 1.7 Hz, 1H, ArH); 1.45 (s, 18H, Bu_t). ^{13}C NMR (400 MHz, $CDCl_3$, δ ppm): 191.5; 154.8; 138.4; 138.1; 131.2; 128.3; 123.9; 34.5; 31.2; 31.0. MALDI-TOF (positive mode, cyano-4-hydroxycinnamic acid as matrix): m/z 235.04 $(M + H)^+$ (100%), calculated 234.20 for $C_{15}H_{22}O_2$.

General method for synthesis of pyrrolidino[60]fullerenes 1, 2 and 3:[24,25]. [60]Fullerene (0.308 g, 0.42 mmol, 2 equiv.), *N*-methylglycine (0.192 g, 2.13 mmol, 10 equiv.) and the suitable benzaldehyde (0.21 mmol, 1 equiv.) in toluene were heated at reflux under a nitrogen atmosphere for 24 h. The solvent was evaporated at reduced pressure and the residue was suspended in 30% carbon disulfide in toluene. The suspension was filtered through a pad of silica and the filtrate was evaporated at reduced pressure. The crude product was purified by column chromatography on silica using a gradient mixture of carbon disulfide, toluene, and hexanes (from 1 : 1 : 4 to 1 : 1 : 1, v/v) as the eluent. The product was recrystallized from carbon disulfide–methanol to afford the final pyrrolidino[60]fullerene as a solid brown powder.

***N*-methyl-3,4-[60]-fullero-2-(3′,5′-di-*tert*-butyl-2′-hydroxyphenyl) pyrrolidino 1.** Following the general procedure, the title compound was isolated as a brown solid in 57% yield (0.12 g). ^{1}H NMR (400 MHz, CS_2/$CDCl_3$, δ ppm): 11.33 (s, 1H, OH); 7.13 (brm, 2H, ArH+ ArH); 5.07 (s, 1H, NCH); 5.05 (d, J = 10 Hz, 1H, NCH_2); 4.27 (d, J = 10 Hz, 1H, NCH_2); 3.03 (s, 3H, NCH_3); 1.31 (s, 18H, Bu_t). MALDI-TOF (positive mode, terthiophene as matrix): m/z 981.9 $(M)^+$ (100%), calculated 981.21 for $C_{77}H_{27}NO$. UV-Vis (CH_2Cl_2): 256, 309, 430, 702 nm.

***N*-methyl-3,4-[60]-fullero-2-(3′,5′-di-*tert*-butyl-4′-hydroxyphenyl) pyrrolidine 2.** Following the general procedure, the title compound was isolated as a brown solid in 55% yield (0.115 g). ^{1}H NMR (400 MHz, CS_2/$CDCl_3$, δ ppm): 7.50 (brs, 2H, ArH); 5.09 (s, 1H, NCH); 4.93 (d, J = 9.3 Hz, 1H, NCH_2); 4.81 (s, 1H, OH); 4.23 (d, J = 9.3 Hz, 1H, NCH_2); 2.82 (s, 3H, NCH_3); 1.37 (s, 18H, Bu_t). MALDI-TOF (positive mode, terthiophene as matrix): m/z 981.20 $(M)^+$ (100%), calculated 981.21 for $C_{77}H_{27}NO$. UV-Vis (CH_2Cl_2): 257, 307, 431, 706 nm.

***N*-methyl-3,4-[60]-fullero-2-(3′,5′-di-*tert*-butylphenyl)pyrrolidine 3.** Following the general procedure, the title compound was isolated as a brown solid in 58% yield (0.115 g). ^{1}H NMR (400 MHz, CS_2/$CDCl_3$, δ ppm): 7.56 (brs, 2H, ArH); 7.24 (d, J = 1.6 Hz, 1H, ArH); 4.95 (d, J = 9.3 Hz, 1H, NCH_2); 4.89 (s, 1H, NCH); 4.26 (d, J = 9.3 Hz, 1H, NCH_2); 2.84 (s, 3H, NCH_3); 1.26 (s, 18H, $(CH_3)_3$). MALDI-TOF (positive mode, terthiophene as matrix): m/z 965.20 $(M)^+$ (100%), calculated 965.21 for $C_{77}H_{27}N$. UV-Vis (CH_2Cl_2): 256, 307, 431, 702 nm.

3 Results

Molecular structures of the phenol–pyrrolidinofullerenes and the model phenyl–pyrrolidinofullerene studied in this work are presented in Fig. 1. All compounds were synthesized from commercially available materials, using the Duff formylation protocol[23] to prepare the appropriate benzaldehyde precursors, followed by the Prato reaction using *N*-methylglycine (sarcosine) in toluene at reflux[24–26] (for details, see Experimental section).

The presence of an intramolecular hydrogen bond in **1** is supported by ^{1}H NMR spectroscopy (Fig. 2), with the OH resonance appearing at δ = 11.33 ppm in a 1 : 1 (v/v) chloroform-*d*–carbon disulfide mixture. By comparison, the OH resonance of **2** appears at δ = 4.81 ppm in the same solvent mixture. The resonance of the methyl group directly attached to the nitrogen in the pyrrolidine ring in **1** (δ = 3.03 ppm) is shifted downfield by $\Delta\delta$ = 0.21 ppm compared to that of **2** (δ = 2.82 ppm). This is ascribed to the deshielding effect induced by the hydrogen-bonded phenolic proton, which decreases the electron density at the nitrogen atom.

In the solid state, the presence of an intramolecular hydrogen bond is supported by the absence of the characteristic free OH vibration (ν = 3640 cm^{-1}) in the FTIR spectrum of **1**, which is clearly observed as a sharp band in the *para*-substituted compound **2** (Fig. 3). Instead, a broad band centered at ν ~ 3100 cm^{-1} is observed in the case of **1**. Congruently, neither of these features is observed in the phenyl derivative, **3**, which lacks the phenolic functional group.

The absorption spectra of **1** and **2** are dominated by features associated with the fullerene[27,28] and are very similar to that of model compound **3**, which lacks the phenolic group (Fig. 4). Visible excitation (400 nm) of compound **3** in dichloromethane results in an emission spectrum with maxima at 716 nm and 791 nm (Fig. 4). Similar emission wavelengths are observed in

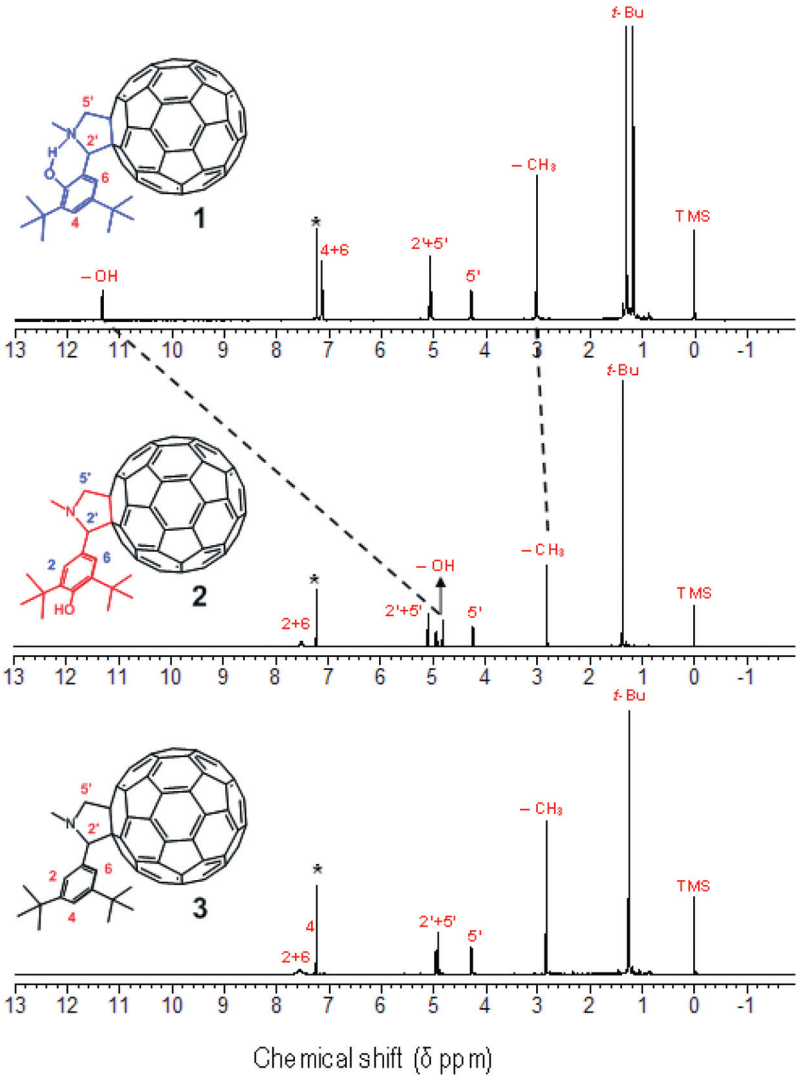

Fig. 2 ^{1}H NMR spectra (400 MHz, 25 °C) of compounds **1**, **2** and **3** in a chloroform-*d*–carbon disulfide mixture (1 : 1, v/v). The downfield shifts observed for the phenolic proton and the methyl group resonances in **1** compared to **2** are attributed to an intramolecular hydrogen bond between the phenol and the pyrrolidine moieties. Peaks marked with an asterisk are due to residual chloroform.

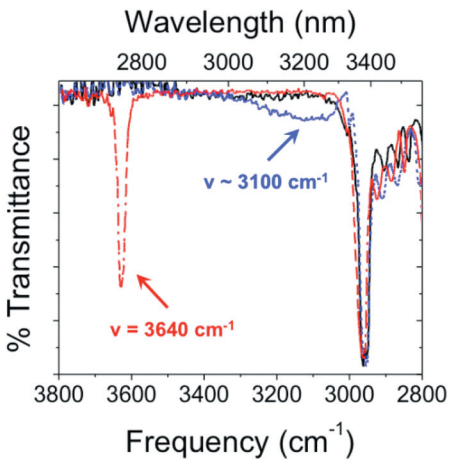

Fig. 3 FTIR spectra of compounds **1** (blue dash), **2** (red dash dot), and **3** (black).

2. However, the fullerene singlet-excited-state lifetime of **1** (τ = 0.26 ns, 97%) in benzonitrile, is significantly shorter then that observed in **2** and **3** (in both cases τ = 1.34 ns) in the same solvent (Fig. 5).[28] In toluene, a non-polar aprotic solvent that destabilizes charge-separated species,[29] the singlet-excited-state lifetime of **1** (τ = 1.01 ns) is similar to that of **2** and **3**. The addition of excess TFA to a benzonitrile solution of **1** presumably gives rise to the protonated form, **4**. Fitting of the fluorescence decay from the acidified solution reveals a bi-exponential decay with a major component of 1.40 ns (60%) attributed to **4** and a minor component of 0.26 ns (30%) assigned to residual **1**. Protonation of the basic pyrrolidino nitrogen presumably disrupts the intramolecular hydrogen bond, leading to the change in lifetime of the fullerene excited-singlet state. Neutralization of the acidic solution with base (tetramethylammonium hydroxide) restores the 0.26 ns component; showing that loss of the short-lived component upon acid titration is not a result of decomposition.

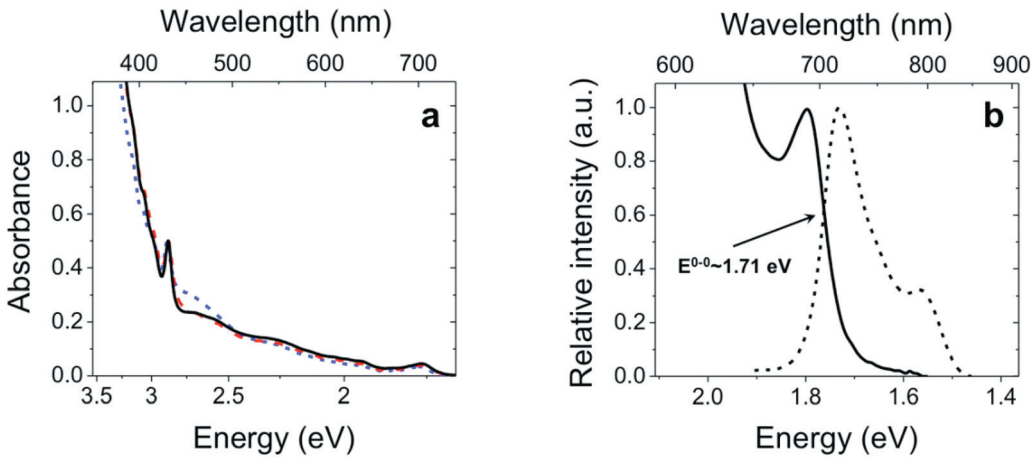

Fig. 4 (a) Normalized steady-state absorption of **1** (blue dash), **2** (red dash dot) and **3** (black); as well as, (b) the normalized steady-state absorption (black) and emission (black dash) of model compound **3** in dichloromethane at room temperature.

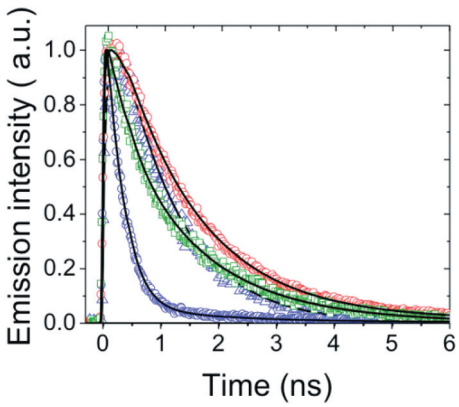

Fig. 5 Time-resolved fluorescence single-photon counting (SPC) measurements of compound **1** in benzonitrile (blue circles), compound **2** in benzonitrile (red circles), compound **1** in toluene (blue triangles); and compound **1** in benzonitrile acidified with TFA to form compound **4** (green triangles). Kinetic fitting of the data (solid lines) shows that in benzonitrile the fullerene singlet-excited state of **1** (τ = 0.26 ns, 97%) is significantly shorter-lived than that of the *para* analog **2** (τ = 1.34 ns) or the protonated form of **1**.

Electrochemical studies (*vs*. SCE) of **1** and **2** reveal two chemically reversible reductions in the potential range investigated (E_m = −0.58 V and −0.98 V for **1** and E_m = −0.58 V and −0.99 V for **2**), characteristic of mono-pyrrolidino-functionalized C_{60} (Fig. 6 and Table 1).[26,27,30] An irreversible oxidation, assigned to the phenoxyl radical–phenol couple, was also observed in these compounds. For **1**, the first oxidation is 0.24 V lower than that observed in **2** (E_p = +1.17 V for **1**, and E_p = +1.41 V for **2**). Electrochemical measurements also show that the addition of sufficient trifluoroacetic acid (up to 425 mM) to a benzonitrile solution of **1** anodically shifts the phenoxyl–phenol couple to a range outside of the observable electrochemical window. The addition of TFA to a solution of **1** presumably shifts the acid–base equilibrium to favor protonation of the basic nitrogen, disrupting the associated hydrogen bond and thus altering the energetics of the phenolic donor. Protonation also affects the potential of the fullerene acceptor.[31] In 425 mM TFA in benzonitrile, the potential of the C_{60}–C_{60}^- couple is −0.46 V.

4 Discussion

In the ^{1}H NMR spectra, the chemical shift of the OH resonance yields information regarding the local electronic environment

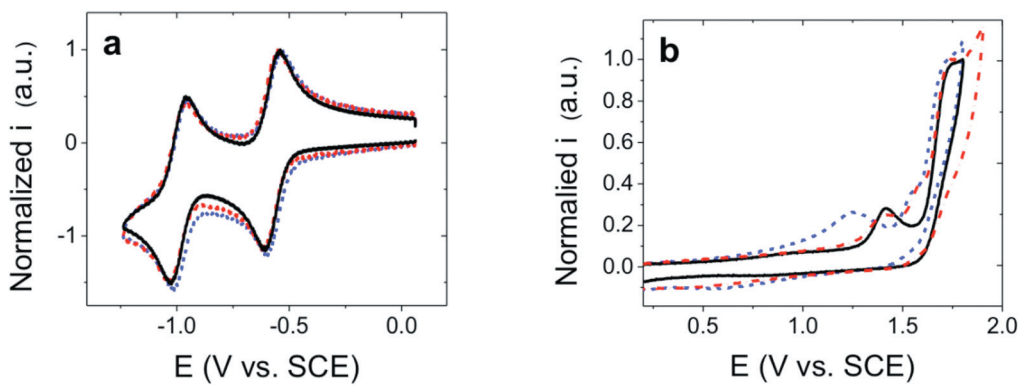

Fig. 6 Cyclic voltammograms of **1** (blue dash), **2** (red dash dot) and **3** (black) recorded in a 0.1 M $TBAPF_6$ benzonitrile solution at a scan rate of 100 mV s^{-1}, with a platinum disk working electrode at room temperature at potentials negative (a) and positive (b) of the SCE reference potential.

Table 1 Redox potentials (V *vs.* SCE) for oxidation (^{ni}E) and reduction (^{n}E) of compounds **1–3**, as determined by cyclic voltammetry. In all cases the electrolyte was 0.1 M tetrabutylammonium hexafluorophosphate in benzonitrile, and the scan rate was 100 mV s^{-1}

Compound	^{II}E	^{I}E	^{i}E	^{ii}E	^{iii}E
1	−0.58[a]	−0.98[a]	1.17[b]	1.57[b]	1.70[b]
2	−0.58[a]	−0.99[a]	1.41[b]	1.59[b]	1.72[b]
3	−0.57[a]	−0.97[a]		1.40[b]	1.72[b]

[a] $E = E_{1/2}$; reversible or quasi-reversible. [b] $E = E_{peak}$; irreversible.

including the relative strength of hydrogen bonds. A stronger hydrogen bond is typically associated with a larger downfield shift.[16a] For compound **1**, the OH resonance is observed at 11.33 ppm, consistent with the formation of the predicted hydrogen bond. For comparison, the phenolic proton resonance of compound **2** appears at a value that is typical of the OH functional group in a non-hydrogen bonding environment (4.81 ppm). However, the resonance of the OH group in **1** is not as far downfield as has been observed in other systems where a phenol is hydrogen bonded to an adjacent imidazole (δ > 13 ppm)[15b,16,21] or pyridine (δ > 14 ppm)[16,20] unit, suggesting a relatively weaker hydrogen bond in the present system.

In many cases, the relative strength of a hydrogen bond is correlated with the pK_a of the protonated associated base.[16] For **1**, the electron-withdrawing and steric effects of the attached fullerene significantly decrease the effective pK_a of the pyrrolidinium ring.[26–28,30] Accordingly, the potential of the phenoxyl radical–phenol couple of **1** (E_p = +1.17 V *vs.* SCE) is significantly higher than those reported for similar phenolic species featuring an intramolecular hydrogen bond to a covalently-attached pyrrolidine ring lacking the C_{60} functionality (E_m = +0.65 V *vs.* SCE).[17b] However, the potential of the phenoxyl radical–phenol couple associated with **1** is still considerably lower (ΔE = 0.24 V) than that observed in the *para* analog **2** (E_p = +1.41 V *vs.* SCE, Fig. 7). This difference in potential can be partially explained in terms of the stabilizing energy of the intramolecular hydrogen bond in **1**. However, the irreversible electrochemical features observed in **1** and **2** suggest that phenolic proton is ultimately transferred to the bulk.

Despite the relatively weak pyrrolidinofullerene base, in the presence of the intramolecular hydrogen bond the fullerene excited-singlet state (E^{0-0} ~ 1.76 eV)[26,28] is thermodynamically capable of photo-oxidizing the attached phenol in **1** ($\Delta G_{ET} \approx$ −40 meV) (Fig. 7). This is not the case for **2** ($\Delta G_{ET} \approx$ +200 meV), which lacks the built in hydrogen bond. Similarly, for the acidified form of **1** (compound **4**) the fullerene excited-singlet state is incapable of oxidizing the phenol moiety. The C_{60} excited-state lifetimes are consistent with these redox thermodynamics. The excited-state lifetime of **1** in benzonitrile (τ = 0.26 ns) is significantly shorter than that observed in **2** and **3** (τ = 1.34 ns for both) in the same solvent, and the quenching is ascribed to photoinduced electron transfer to the fullerene to yield a transient charge-separated state. This conclusion is supported by the fact that the excited-state lifetime of **1** is restored to a more typical value in toluene (Fig. 5); a less polar solvent that destabilizes charge-separated species, thereby reducing the driving force for and rate of photoinduced electron transfer.[29] Furthermore, the excited-state lifetime quenching is eliminated when the hydrogen bond is disrupted by the addition of an exogenous acid (TFA) to yield **4** (Fig. 5). The relative stability of the fullerene unit in this architecture allows for investigation of these compounds under acidic conditions. Similar studies were prohibited when using our previously reported porphyrin based photochemical system,[21b] due to the higher pK_a of the protonated pyrrole nitrogens on the porphyrin macrocycle. These results indicate that in addition to the ionizable phenolic proton, the protonation state of the pendant base can also influence the redox properties of a photochemically active redox pair.

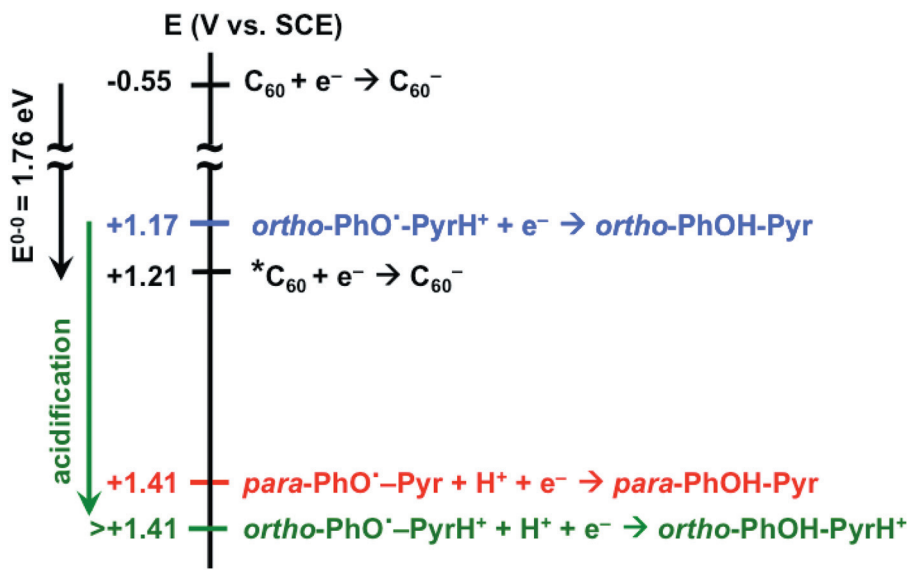

Fig. 7 Energy level diagram including the $E_{1/2}$ of the C_{60}–C_{60}^- and $^*C_{60}$–C_{60}^- processes (black), E_p for phenoxyl–phenol couple of **1** (blue), and the effect of acidification (which shifts the phenoxyl–phenol couple outside of the electrochemical window) (green), as well as E_p for the phenoxyl–phenol couple of **2** (red).

5 Conclusion

Our optical and electrochemical investigations show that in addition to using the pyrrolidinofullerene as an electron acceptor, the pyrrolidino nitrogen can be used as a built in proton-accepting unit that modulates the energetics of the attached donor. The system mimics certain aspects of PCET reactions in biology and thus provides a model for better understanding the role of this class of reactions in forming efficient interfaces between light absorbing reaction centers and multi-electron catalytic components.

References

1 B. A. Barry, Proton coupled electron transfer and redox active tyrosines in photosystem II, *J. Photochem. Photobiol. B*, 2011, **104**, 60–71.

2 J. L. Dempsey, J. R. Winkler and H. B. Gray, Proton-coupled electron flow in protein redox machines, *Chem. Rev.*, 2010, **110**, 7024–7039.

3 J. P. McEvoy and G. W. Brudvig, Water-splitting chemistry of photosystem II, *Chem. Rev.*, 2006, **106**, 4455–4483.

4 J. Stubbe, D. G. Nocera, C. S. Yee and M. C. Y. Chang, Radical initiation in the class I Ribonucleotide Reductase: Long-range proton-coupled electron transfer?, *Chem. Rev.*, 2003, **103**, 2167–2201.

5 S. Ferguson-Miller and G. T. Babcock, Heme/copper terminal oxidases, *Chem. Rev.*, 1996, **96**, 2889–2908.

6 C. Costentin, M. Robert and J.-M. Savéant, Concerted proton–electron transfers in the oxidation of phenols, *Phys. Chem. Chem. Phys.*, 2010, **12**, 11179–11190.

7 C. Costentin, Electrochemical approach to the mechanistic study of proton-coupled electron transfer, *Chem. Rev.*, 2008, **108**, 2145–2179.

8 J. M. Mayer, Simple marcus-theory-type model for hydrogen-atom transfer/proton-coupled electron transfer, *J. Phys. Chem. Lett.*, 2011, **2**, 1481–1489.

9 S. Hammes-Schiffer, Current theoretical challenges in proton-coupled electron transfer: Electron-proton nonadiabaticity, proton relays, and ultrafast dynamics, *J. Phys. Chem. Lett.*, 2011, **2**, 1410–1416.

10 C. J. Gagliardi, B. C. Westlake, C. A. Kent, J. J. Paul, J. M. Papanikolas and T. J. Meyer, Integrating proton coupled electron transfer (PCET) and excited states, *Coord. Chem. Rev.*, 2010, **254**, 2459–2471.

11 M. H. V. Huynh and T. J. Meyer, Proton-coupled electron transfer, *Chem. Rev.*, 2007, **107**, 5004–5064.

12 J. Rosenthal and D. G. Nocera, Role of proton-coupled electron transfer in O–O bond activation, *Acc. Chem. Res.*, 2007, **40**, 543–553.

13 J. M. Mayer, Proton-coupled electron transfer: A reaction chemist's view, *Annu. Rev. Phys. Chem.*, 2004, **55**, 363–390.

14 Y. Umena, K. Kawakami, J.-R. Shen and N. Kamiya, Crystal structure of oxygen-evolving photosystem II at a resolution of 1.9 Å, *Nature*, 2011, **473**, 55–60.

15 (*a*) M.-T. Zhang and L. Hammarström, Proton-coupled electron transfer from tryptophan: A concerted mechanism with water as proton acceptor, *J. Am. Chem. Soc.*, 2011, **133**, 13224–12227; (*b*) M.-T. Zhang, T. Irebo, O. Johansson and L. Hammarström, Proton coupled electron transfer from tyrosine: A strong rate dependence on intramolecular proton transfer distance, *J. Am. Chem. Soc.*, 2011, **133**, 8806–8809; (*c*) T. Irebo, O. Johansson and L. Hammarström, The rate ladder of proton-coupled tyrosine oxidation in water: A systematic dependence on hydrogen bonds and protonation state, *J. Am. Chem. Soc.*, 2009, **130**, 9194–9195; (*d*) L. Johannissen, T. Irebo, M. Sjödin, O. Johansson and L. Hammarström, The kinetic effect of internal hydrogen bonds on proton-coupled electron transfer from phenols: A theoretical analysis with modeling of experimental data, *J. Phys. Chem. B*, 2009, **113**, 16214–16225; (*e*) M. Sjödin, T. Irebo, E. Utas Josefin, J. Lind, G. Merenyi, B. Åkermark and L. Hammarström, Kinetic effects of hydrogen bonds on proton-coupled electron transfer from phenols, *J. Am. Chem. Soc.*, 2006, **128**, 13076–13083; (*f*) L. Sun, M. Burkitt, M. Tamm, M. K. Raymond, M. Abrahamsson, D. LeGourriérec, Y. Frapart, A. Magnuson, P. H. Kenéz, P. Brandt, A. Tran, L. Hammarström, S. Styring and B. Åkermark, Hydrogen-bond promoted intramolecular electron transfer to photogenerated Ru(III): A functional mimic of $Tyrosine_Z$ and Histidine 190 in Photosystem II, *J. Am. Chem. Soc.*, 1999, **121**, 6834–6842.

16 (*a*) T. F. Markle, I. J. Rhile, A. G. Dipasquale and J. M. Mayer, Probing concerted proton– electron transfer in phenol–imidazoles, *Proc. Natl. Acad. Sci. USA*, 2008, **105**, 8185–8190; (*b*) T. F. Markle and J. M. Mayer, Concerted proton–electron transfer in pyridylphenols: The importance of the hydrogen bond, *Angew. Chem., Int. Ed.*, 2008, **47**, 738–740; (*c*) I. J. Rhile, T. F. Markle, H. Nagao, A. G. Dipasquale, O. P. Lam, M. A. Lockwood, K. Rotter and J. M. Mayer, Concerted proton −electron transfer in the oxidation of hydrogen-bonded phenols, *J. Am. Chem. Soc.*, 2006, **128**, 6075–6088; (*d*) I. J. Rhile and J. M. Mayer, One-electron oxidation of a hydrogen-bonded phenol occurs by concerted proton-coupled electron transfer, *J. Am. Chem. Soc.*, 2004, **126**, 12718–12719.

17 (*a*) C. Costentin, M. Robert and J.-M. Savéant, Adiabatic and non-adiabatic concerted proton−electron transfers. Temperature effects in the oxidation of intramolecularly hydrogen-bonded phenols, *J. Am. Chem. Soc.*, 2007, **129**, 9953–9963; (*b*) C. Costentin, M. Robert and J.-M. Savéant, Electrochemical and homogeneous proton-coupled electron transfers: Concerted pathways in the one-electron oxidation of a phenol coupled with an intramolecular amine-driven proton transfer, *J. Am. Chem. Soc.*, 2006, **128**, 4552–4553.

18 (*a*) C. J. Fecenko, H. H. Thorp and T. J. Meyer, The role of free energy change in coupled electron-proton transfer, *J. Am. Chem. Soc.*, 2007, **129**, 15098–15099; (*b*) J. J. Concepcion, M. K. Brennaman, J. R. Deyton, N. V. Lebedeva, M. D. E. Forbes, J. M. Papanikolas and T. J. Meyer, Excited-state quenching by proton-coupled electron transfer, *J. Am. Chem. Soc.*, 2007, **129**, 6968–6969.

19 (*a*) L. Benisvy, R. Bittl, E. Bothe, C. D. Garner, J. McMaster, S. Ross, C. Teutloff and F. Neese, Phenoxyl radicals hydrogen-bonded to imidazolium: Analogues of tyrosyl D• of Photosystem II: High-field EPR and DFT studies, *Angew. Chem., Int. Ed.*, 2005, **44**, 5314–5317; (*b*) F. Lachaud, A. Quaranta, Y. Pellegrin, P. Dorlet, M. F. Charlot, S. Un, W. Liebl and A. Aukauloo, A. biomimetic model of the electron transfer between P680 and the TyrZ–His190 pair of PSII, *Angew. Chem., Int. Ed.*, 2005, **44**, 1536–1540; (*c*) L. Benisvy, E. Bill, A. J. Blake, D. Collison, E. S. Davies, C. D. Garner, C. I. Guindy, E. J. L. McInnes, G. McArdle, J. McMaster, C. Wilson and J. Wolowska, Phenolate and phenoxyl radical complexes of Co(II) and Co(III), *Dalton Trans.*, 2004, 3647–3653. Q4

20 L. Biczók, N. Gupta and H. Linschitz, Coupled electron-proton transfer in interactions of Triplet C_{60} with hydrogen-bonded phenols: Effects of solvation, deuteration, and redox potentials, *J. Am. Chem. Soc.*, 1997, **119**, 12601–12609.

21 (*a*) G. F. Moore, M. Hambourger, M. Gervaldo, O. G. Poluektov, T. Rajh, D. Gust, T. A. Moore and A. L. Moore, A bioinspired construct that mimics the proton coupled electron transfer between P680+ and the TyrZ-His190 pair of Photosystem II, *J. Am. Chem. Soc.*, 2008, **130**, 10466–10467; (*b*) G. F. Moore, M. Hambourger, G. Kodis, W. Michl, D. Gust, T. A. Moore and A. L. Moore, Effects of protonation state on a Tyrosine-Histidine bioinspired redox mediator, *J. Phys. Chem. B*, 2010, **114**, 14450–14457.

22 D. Gust, T. A. Moore, D. K. Luttrull, G. R. Seely, E. Bittersman, R. V. Bensasson, M. Rougee, E. J. Land, S. F. C. De and D. A. M. Van, Photophysical properties of 2-nitro-5,10,15,20-tetra-p-tolylporphyrins, *Photochem. Photobiol.*, 1990, **51**, 419–426.

23 J. F. Larrow and E. N. Jacobsen, A practical method for the large-scale preparation of [N,N′-bis(3,5-di-tert-butylsalicy1idene)-1,2-cyclohexanediaminato(2-)] manganese(III) chloride, a highly enantioselective epoxidation catalyst, *J. Org. Chem.*, 1994, **59**, 1939–1942.

24 M. Maggini, G. Scorrano and M. Prato, Addition of azomethine ylides to C_{60}: synthesis, characterization, and functionalization of fullerene pyrrolidines, *J. Am. Chem. Soc.*, 1993, **115**, 9798–9799.

25 I. A. Nuretdinov, V. P. Gubskaya, V. V. Yanilkin, V. I. Morozov, V. V. Zverev, A. V. Il'yasov, G. M. Fazleeva, N. V. Nastapova and D. V. Il'matova, Fulleropyrrolidine-containing sterically hindered phenol. Synthesis, structure and properties, *Russ. Chem. Bull.*, 2001, **50**, 607–613.

26 M. Prato and M. Maggini, Fulleropyrrolidines: A family of full-fledged fullerene derivatives, *Acc. Chem. Res.*, 1998, **31**, 519–526.

27 A. Hirsch and M. Brettreich, *Fullerenes*, Wiley-VCH, Weinheim, Germany, 2005.

28 D. M. Guldi and M. Prato, Excited-state properties of C60 fullerene derivatives, *Acc. Chem. Res.*, 2000, **33**, 695–703.

29 D. Gust, T. A. Moore and A. L. Moore, Mimicking photosynthetic solar energy transduction, *Acc. Chem. Res.*, 2001, **34**, 40–48.

30 L. Echegoyen and L. E. Echegoyen, Electrochemistry of fullerenes and their derivatives, *Acc. Chem. Res.*, 1998, **31**, 593–601.

31 (*a*) Y. Sun, B. Ma and C. E. Bunker, Photoinduced Intramolecular n–π* Electron Transfer in Aminofullerene Derivatives, *J. Phys. Chem. A*, 1998, **102**, 7580–7590; (*b*) Y. Sun, B. Ma and C. E. Bunker, Photoinduced Intramolecular n–π* Electron Transfer in Aminofullerene Derivatives, *J. Phys. Chem. A*, 1998, **102**, 7580–7590; (*c*) N. Armaroli, G. Accorsi, J. Gisselbrecht, M. Gross, V. Krasnikov, D. Tsamouras, G. Hadziioannou, M. J. Gómez-Escalonilla, F. Langa, J. Eckert and J. Nierengarten, Photoinduced processes in fullerenepyrrolidine and fullerenopyrazoline derivatives substituted with an oligophenylenevinylene moiety, *J. Mater. Chem.*, 2002, **12**, 2077–2087.

